Nucleic acid scavengers inhibit thrombosis without increasing bleeding

Shashank Jain[a], George A. Pitoc[a], Eda K. Holl[a], Ying Zhang[b], Luke Borst[c], Kam W. Leong[b], Jaewoo Lee[a], and Bruce A. Sullenger[a,1]

[a]Department of Surgery, Duke University Medical Center, Durham, NC 27710; [b]Department of Biomedical Engineering, Duke University, Durham, NC 27708; and [c]Department of Pathology, North Carolina State University College of Veterinary Medicine, Raleigh, NC 27607

Edited by Robert Langer, Massachusetts Institute of Technology, Cambridge, MA, and approved July 4, 2012 (received for review March 23, 2012)

Development of effective, yet safe, antithrombotic agents has been challenging because such agents increase the propensity of patients to bleed. Recently, naturally occurring polyphosphates such as extracellular DNA, RNA, and inorganic polyphosphates have been shown to activate blood coagulation. In this report, we evaluate the anticoagulant and antithrombotic activity of nucleic acid-binding polymers in vitro and in vivo. Such polymers bind to DNA, RNA, and inorganic polyphosphate molecules with high affinity and inhibit RNA- and polyphosphate-induced clotting and the activation of the intrinsic pathway of coagulation in vitro. Moreover, $[NH_2(CH_2)_2NH_2]:(G=3)$;dendri PAMAM$(NH_2)_{32}$ (PAMAM G-3) prevents thrombosis following carotid artery injury and pulmonary thromboembolism in mice without significantly increasing blood loss from surgically challenged animals. These studies indicate that nucleic acid-binding polymers are able to scavenge effectively prothrombotic nucleic acids and other polyphosphates in vivo and represent a new and potentially safer class of antithrombotic agents.

polyphosphates/DNA/RNA | platelet | hemorrhage

Thrombosis remains one of the leading causes of death and disability in the Western world despite the development of various anticoagulants for treatment of deep vein thrombosis, stroke, atherosclerosis, and other cardiovascular diseases, cardiac interventions, and metastatic cancers (1–3). Thrombotic episodes during these conditions can be managed by various antithrombotic and anticoagulant drugs, which can also produce moderate to severe side effects (2, 4–7). Hence, development of an effective, yet safe, anticoagulant remains a long-sought objective. Recently, naturally occurring polyphosphates such as extracellular RNA, DNA, and inorganic polyphosphates have been reported to be potent activators of the coagulation cascade. Extracellular RNA activates coagulation though activation of factors XII and XI in vitro and in vivo (8). In addition, extracellular RNA has also been found to act as cofactor for the activation of factor VII-activating protease (FSAP) (9). DNA-rich neutrophil extracellular traps (NET) have been found to promote thrombosis (10). Inorganic polyphosphates, which are stored in dense bodies of mammalian platelets and secreted on platelet activation, can activate the contact pathway of coagulation and strengthen fibrin clots. Polyphosphates have been shown to accelerate factor XI activation by thrombin and factor Xa (11). Polyphosphates can also inhibit the activity of tissue factor pathway inhibitor (TFPI) and accelerate the activity of thrombin-activatable fibrinolysis inhibitor (TAFI) (12, 13). In the blood of hemophilia A and B patients and Hermansky-Pudlak syndrome patients, polyphosphates significantly reduce the clotting times (14). Moreover, platelet polyphosphates have also been reported to be proinflammatory and polyphosphate-factor XII binding results in the release of the inflammatory mediator bradykinin by plasma kallikrein-mediated kininogen processing (14). Taken together, all these observations suggest that naturally occurring polyphosphates such as extracellular DNA, RNA, and inorganic polyphosphate are potent activators of the coagulation cascade and represent a potential therapeutic target for novel anticoagulation strategies.

Recently, we discovered that nucleic acid-binding polymers (NABPs) can act as molecular scavengers and counteract the activity of any nucleic acid aptamer regardless of its sequence, as well as inhibit RNA- and DNA-mediated activation of Toll-like receptors (TLRs) and inflammation (15, 16). The observations that nucleic acids and other polyphosphates are involved in thrombosis led us to hypothesize that such scavengers may also be able to inhibit polyphosphate-mediated thrombosis. Therefore, we sought polymers that could bind all of these classes of polyphosphates with high affinity. In this report, we screened a wide variety of nucleic acid polymers using in vitro clotting assays for their potential to inhibit activation of coagulation cascade and to identify the best suitable NABP to act as a potent and safe anticoagulant and antithrombotic agent. Based on the results of in vitro experiments, we explored the anticoagulant and antithrombotic properties of a widely used NABP: generation-3 PAMAM G-3, $[NH_2(CH_2)_2NH_2]:(G=3)$;dendri PAMAM$(NH_2)_{32}$. PAMAM G-3 is a polycationic polyamine polymer (MW 6909) with a core of 1,4-diaminobutane. It has a diameter of 36 Å with the 32 surface amine groups (17). It has a high degree of molecular uniformity, narrow molecular weight distribution, well-defined size and shape characteristics, and a highly functionalized terminal surface (18). Because of these characteristics, PAMAM has been proven to be extremely useful for a variety of applications, such as gene therapy, molecular diagnostics, controlled drug delivery, and imaging, in the field of biomedical sciences (17, 18).

Results

Nucleic Acid-Binding Polymers Inhibit Polyphosphate-Mediated Coagulation in Vitro. As previously described, inorganic polyphosphates (PolyP) act as strong activators of the coagulation cascade and can replace the routinely used activator, kaolin, in standard blood clotting assays (19). We utilized inorganic polyphosphate with the average chain length of 60 and 130 as activators for coagulation cascade to screen different NABP for their anticoagulant activity in vitro. Inorganic polyphosphates 60 and 130 decreased the clotting times of normal pooled human plasma by over 100 s when added at a concentration of 20 μM (Fig. 1). Then, we evaluated the ability of NABP's CDP (β-cyclodextrin–containing polycation), HDMBr (hexadimethrine bromide), PAMAM G-1 (polyamidoamine dendrimer, 1,4-diaminobutane core, generation 1), PAMAM G-3, and PAMAM-G5 to reverse this procoagulant activity of inorganic polyphosphates (Fig. 1). All polymers showed anticoagulant activity in a dose-dependent fashion. At the concentration of 60 μg/mL CDP completely inhibits the inorganic polyphosphate 60- and 130-mediated activa-

Author contributions: S.J., and B.A.S. designed research; S.J., G.A.P., E.K.H., L.B., and Y.Z. performed research; S.J., K.W.L., J.L., L.B., and B.A.S. analyzed data; and S.J. and B.A.S. wrote the paper.

The authors declare no conflict of interest.

This article is a PNAS Direct Submission.

[1]To whom correspondence should be addressed. E-mail: bruce.sullenger@duke.edu.

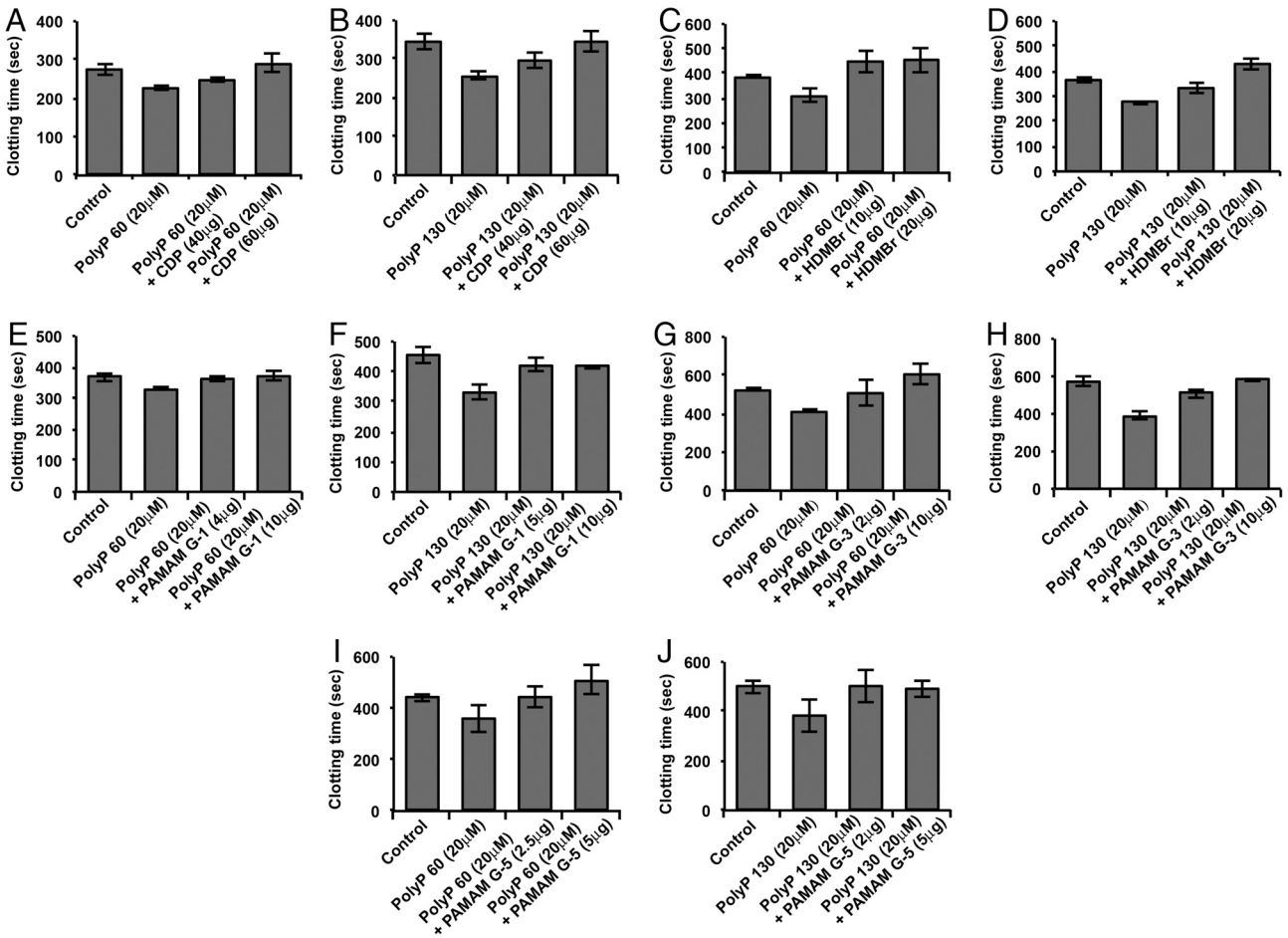

Fig. 1. NABPs inhibit inorganic polyphosphate-mediated clotting in vitro. Normal human pooled plasma was treated with PolyP 60 (20 μg/mL) and PolyP 130 (20 μg/mL). Different NABPs were added in various concentrations and clotting times were recorded using a STart® Hemostasis Analyzer. (*A* and *B*) CDP; (*C* and *D*) HDMBr; (*E* and *F*) PAMAM G-1; (*G* and *H*) PAMAM G-3; and (*I* and *J*) PAMAM G-5. Error bars represent standard deviation.

tion of clotting (Fig. 1 *A* and *B*), whereas HDMBr inhibited inorganic polyphosphate 60- and 130-mediated clotting at the concentrations of 10 μg/mL and 20 μg/mL, respectively (Fig. 1 *C* and *D*). Three different generations of PAMAM (G-1, G-3, and G-5) also displayed significant anticoagulant activity. PAMAM G-1 inhibited polyphosphate 60- and 130-mediated clotting at the concentrations of 4 μg/mL and 10 μg/mL, respectively (Fig. 1 *E* and *F*). At concentrations as low as 2 μg/mL and 2.5 μg/mL both PAMAM G-3 and G-5 were able to reverse the procoagulant effects of PolyP 60 and PolyP 130, respectively (Fig. 1 *G*–*J*). These results demonstrate that NABPs can counteract polyphosphate-mediated activation of coagulation. Although all polymers showed anticoagulant activity in vitro, we chose to focus upon PAMAM G-3 for additional in vitro characterization and in vivo thrombosis studies because, along with PAMAM G-5, it was effective at the lowest concentration and has been reported to have lower toxicity than PAMAM G-5 (20).

PAMAM G-3 Binds with High Affinity to Various Polyphosphates in Vitro. Previously, we reported that a PAMAM G-3 binds to ssRNA, dsRNA, and ssDNA with high affinity (16). Hence, using isothermal titration calorimetry (ITC), we investigated whether PAMAM G-3 binds to inorganic polyphosphates and dsDNA with high affinity. As shown in Tables 1 and 2, we found that PAMAM G-3 binds PolyP 60 with a higher affinity ($K_d = 7.86E{+}08\ M^{-1}$) than ssDNA (CpG) ($K_d = 4.12E{+}08\ M^{-1}$) and dsRNA (Poly I:C) ($K_d = 1.05E{+}08\ M^{-1}$)—the larger the number of phosphates in the inorganic polyphosphate chain (130 versus 60), the higher the affinity. In addition, we observed that PAMAM G-3 binds long dsDNA (plasmid) with a similar high binding affinity ($K_d = 6.41E{+}08\ M^{-1}$) as inorganic polyphosphate 60 ($K_d = 7.86E{+}08\ M^{-1}$). Thus, PAMAM G-3 binds with high affinity to prothrombotic polyphosphates such as DNA, RNA, and inorganic polyphosphates.

PAMAM G-3 Inhibits Activation of the Contact Pathway. In addition to inhibiting PolyP 60- and 130-mediated activation of clotting, PAMAM G-3 also inhibits RNA-mediated (Poly I:C) activation of clotting (Fig. 2*A*), indicating that NABPs can inhibit activation of clotting by various types of extracellular polyphosphates. In addition, we observed that PAMAM G-3 can inhibit activation of the contact pathway of coagulation. In a standard activated

Table 1. Thermodynamic parameters for PAMAM G-3 binding to various polyphosphates (first-stage binding)

Polyanions	N1*	$K_d1^{\dagger}$ (M^{-1})	$\Delta G1^{\ddagger}$ (kJ/mole)	$\Delta H1^{\S}$ (kJ/mole)	$T\Delta S^{\P}$ (kJ/mole)
PolyP 130	0.004	5.85E+09	−2.86	−0.68	2.18
PolyP 60	0.0113	7.86E+08	−2.50	−0.64	1.87
CpG	0.091	4.12E+08	−2.58	−0.57	2.02
Poly I:C	0.127	1.05E+08	−2.78	−1.19	1.59
Plasmid	0.0181	6.41E+08	−2.78	−1.19	1.59

*N: Stoichiometric ratio of nitrogen to phosphorous in polyphosphates;
†K_d: dissociation constant;
‡ΔG: free energy change;
§ΔH: enthalpy change;
¶TΔS: entropy change.

Table 2. Thermodynamic parameters for PAMAM G-3 binding to various polyphosphates (second-stage binding)

Polyanions	N2*	K_d2 (M^{-1})†	ΔG2 (kJ/mole)‡	ΔH2 (kJ/mole)§	TΔS (kJ/mole)¶
PolyP 130	0.0039	8.36E+06	−2.68	0.22	2.91
PolyP 60	0.0.0049	4.97E+06	−1.38	2.55	3.93
CpG	0.0423	1.64E+06	−3.61	−1.04	2.57
Poly I:C	0.0.0607	1.30E+06	3.25	5.83	2.58
Plasmid	0.00482	6.97E+06	−2.23	1.27	3.50

*N: Stoichiometric ratio of nitrogen to phosphorous in polyphosphates;
†K_d: dissociation constant;
‡ΔG: free energy change;
§ΔH: enthalpy change;
¶TΔS: entropy change.

partial thromboplastin time (aPTT) clotting assay, which employs a nonphysiological anionic activator of coagulation kaolin, PAMAM G-3 inhibited clotting in a dose-dependent fashion (Fig. 2*B*). By contrast, PAMAM G-3 did not significantly impact tissue factor-initiated coagulation as measured in a prothrombin time (PT) clotting assay (Fig. 2*C*). These findings indicate that the NABP PAMAM G-3 inhibits activation of the contact or intrinsic pathway of coagulation by polyanions without impacting activation of the extrinsic pathway of coagulation.

To examine the anticoagulant properties of PAMAM G-3 in the more relevant physiological setting of human blood, we evaluated its effect on clotting in thrombelastography (TEG) assays (Fig. 2*D*). Polyphosphate 60 can activate clotting in whole blood as measured in a TEG assay and shorten the lag time (time to start clot formation). The lag time (*R*) in whole blood with polyphosphate 60 (140 μM) was 21.9 min as compared to 27.8 min for whole blood without polyphosphate treatment. Addition of PAMAM G-3 (200 μg/mL) to the blood inhibited the polyphosphate-mediated clot formation and increased lag time from 21.9 min to 64.4 min. PAMAM G-3 also slowed down the rate of clot formation (α) (Fig. 2*E*). All together, these observations show that PAMAM G-3 inhibits the formation of extracellular RNA and inorganic polyphosphate-engendered clots in human plasma and whole blood in vitro.

PAMAM G-3 Inhibits Thrombosis in Vivo. To evaluate the ability of the NABP PAMAM G-3 to inhibit thrombosis in vivo, we utilized two mouse models of thrombosis: the $FeCl_3$-induced carotid artery injury model and collagen/epinephrine-induced pulmonary thromboembolism model. We observed that the mean time for the occlusion of the carotid artery after $FeCl_3$ treatment was 4 min 30 s for control mice treated with saline ($n = 12$). By contrast, none of the vessels in mice treated with PAMAM G-3 (20 mg/kg) were occluded in 5 min, and 11 of the 12 animals showed no occlusion of the carotid artery for greater than 40 min following $FeCl_3$-induced damage (Fig. 3*A*). Only 50% of animals showed patent artery after 40 min following $FeCl_3$-induced damage at a 15 mg/kg dose (Fig. 3*A*). Histological analysis of damaged arteries from $FeCl_3$-challenged animals confirmed that large thrombi had formed in control-treated animals (Fig. 3*B*), although no clot was apparent in PAMAM G-3–treated animals (Fig. 3*C*).

An additional mouse model of thrombosis, collagen/epinephrine-induced lethal pulmonary thromboembolism, was also used to evaluate antithrombotic activity of PAMAM G-3 in vivo in the microvasculature. None of the control-treated (normal saline) mice ($n = 11$) survived beyond 3.5 min after the injection of collagen/epinephrine, although 83% of mice treated with

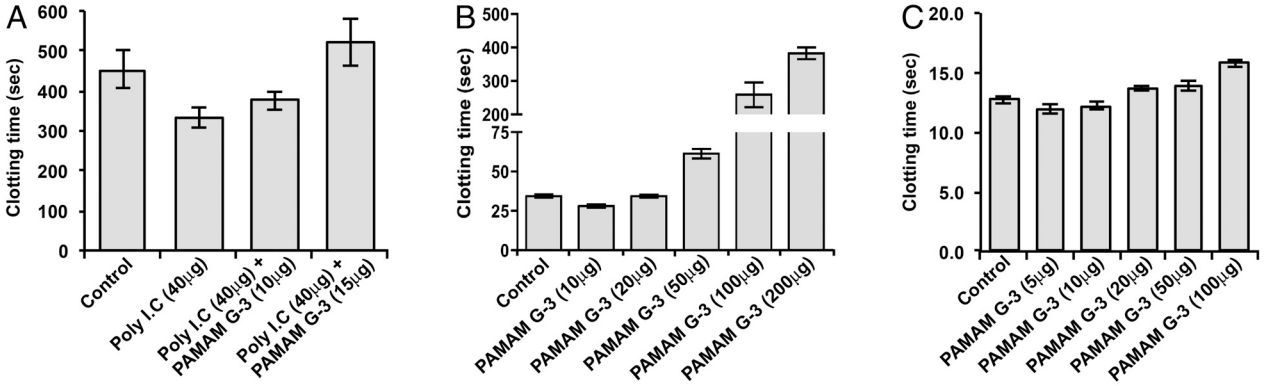

D

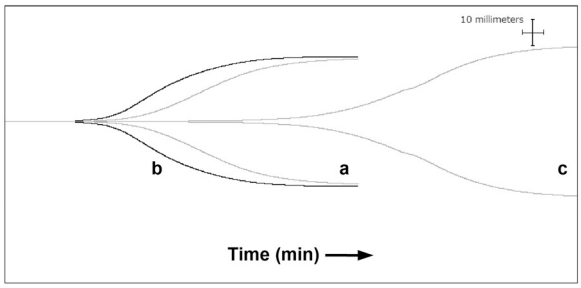

E

	Assay parameter→ ↓Treatment	R (min)	K (min)	α Angle (degree)	MA (mm)
a	Whole blood + PBS (Phosphate-buffered Saline)	27.8	17.2	14.1	45
b	Whole blood + Polyphosphate 60 (140μM)	21.9	12.7	17.4	46.6
c	Whole blood + Polyphosphate 60 (140μM) + PAMAM G-3 (200μg/ml)	64.4	27	9.8	53.4

Fig. 2. Anticoagulant effect of PAMAM G-3. (*A*) Effect of PAMAM G-3 on Poly I:C-mediated clotting in vitro. Normal human pooled plasma was treated with Poly I:C and increasing concentrations of PAMAM G-3 were added. Clotting times were recorded using a STart® Hemostasis Analyzer. (*B*) Effect of PAMAM G-3 on the activation of intrinsic pathway. Normal human pooled plasma was treated with increasing concentrations of PAMAM G-3. aPTT reagent was used to activate intrinsic pathway. Clotting times were recorded using a STart® Hemostasis Analyzer. (*C*) Effect of PAMAM G-3 on the activation of extrinsic pathway. Normal human pooled plasma was treated with increasing concentrations of PAMAM G-3. PT reagent was added to activate extrinsic pathway. Clotting times were recorded using a STart® Hemostasis Analyzer. (*D*) Effect of PAMAM G-3 on clotting in a TEG assay: "a," whole blood without activator; "b," whole blood + PolyP 60 (140 μM); "c," whole blood + PolyP 60 (140 μM) + PAMAM G-3 (200 μg/mL). (*E*) A table showing all coagulation parameters acquired (R, lag time; K, speed to reach a certain level of clot strength; α angle, rapidity of clot strengthening; MA, maximum amplitude, the ultimate strength of the fibrin clot). Error bars represent standard deviation.

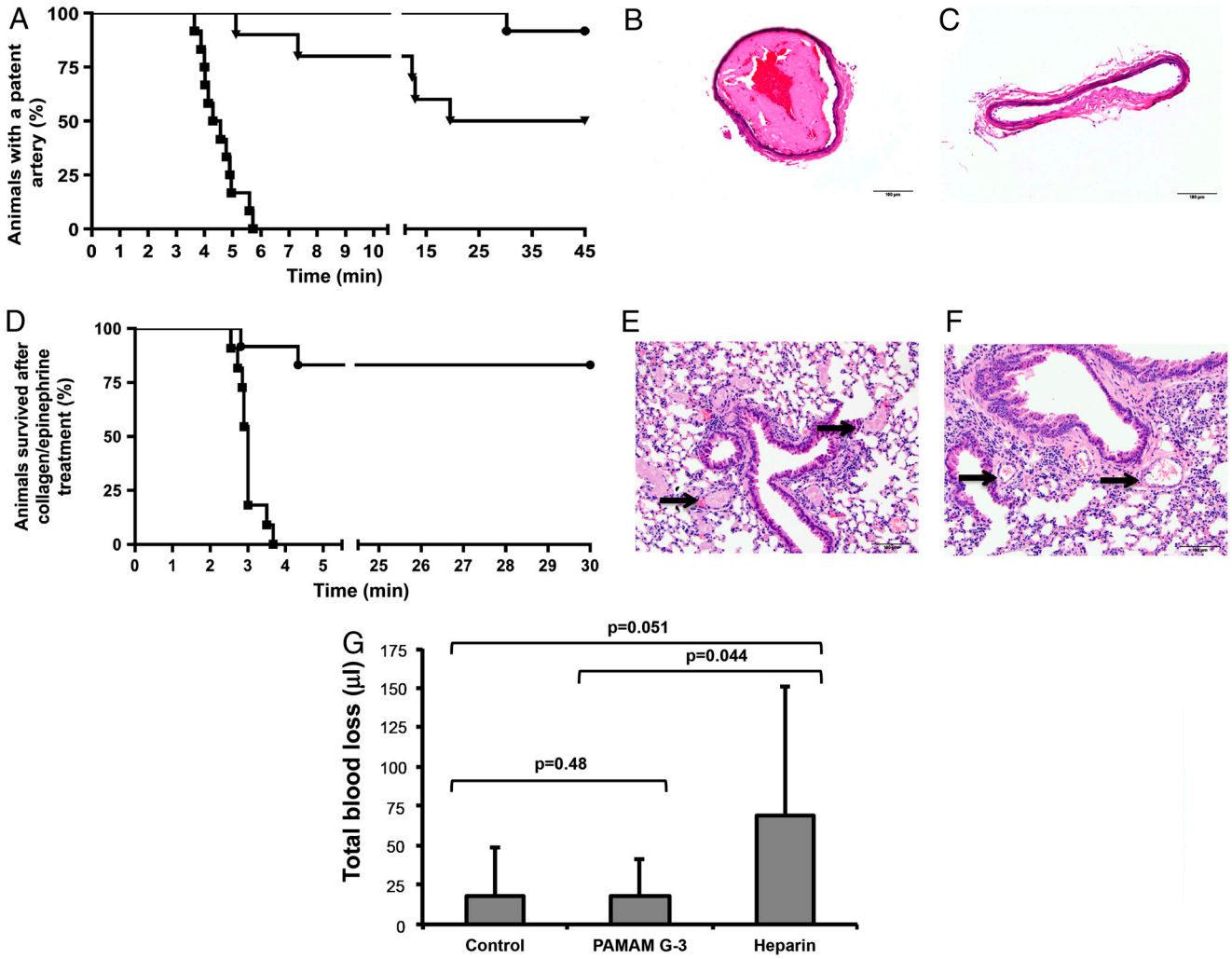

Fig. 3. Effect of PAMAM G-3 on thrombosis and bleeding. FeCl3-induced carotid artery injury: mice were treated with control (normal saline, squares), PAMAM G-3 (15 mg/kg, triangles), and PAMAM G-3 (20 mg/kg, circles). Blood flow was observed in the carotid artery after the treatment with $FeCl_3$, as described in *Materials and Methods*. (*A*) Kaplan-Meier graph showing the percentage of animals with a patent artery after $FeCl_3$-induced injury. Representative H- and E-stained cross-sections of injured carotid artery from mice treated with control (*B*) and PAMAM G-3 (*C*). Collagen/Epinephrine induced pulmonary thromboembolism: (*D*) Kaplan-Meier graph showing the percentage of animals survived after collagen/epinephrine injection. Mice were treated with control (normal saline, squares) or PAMAM G-3 (20 mg/kg, circles) followed by collagen/epinephrine, as described in *Materials and Methods*. Representative H- and E-stained cross-sections of lungs from mice treated with (*E*) control and (*F*) PAMAM G-3. Arrows show the vessels in lung sections. Tail-transection assay: (*G*) Mice were injected with control (normal saline), PAMAM G-3 (20 mg/kg), and heparin (200 U/kg). After 15 min, 3 mm of distal tail were surgically removed and blood loss caused by the injury was monitored over 10 min, as described in *Materials and Methods*. Error bars represent standard deviation.

PAMAM G-3 (20 mg/kg; $n = 12$) survived for more than 30 min after administration of collagen/epinephrine mixture, indicating that PAMAM G-3 also has potent antithrombotic activity in the setting of pulmonary thromboembolism (Fig. 3*D*). Moreover, histological analysis demonstrated that microvessels in the lungs of control-treated animals contain thrombi (arrows in Fig. 3*E*), whereas such vessels in animals treated with PAMAM G-3 were largely patent (arrows in Fig. 3*F*). These observations demonstrate that PAMAM G-3 has a strong antithrombotic effect in two mouse models: a carotid-large artery damage thrombosis model and a pulmonary embolism-microvessel thrombosis model.

PAMAM G-3 Does Not Increase Bleeding. Most of the commonly used antithrombotic agents come with an inherent risk of severe or fatal bleeding (21–24). To assess the effect of PAMAM G-3 administration on bleeding, we surgically challenged mice treated with the NABP PAMAM G-3 by tail transection and monitored blood loss. We evaluated the effect of intravenous treatment of PAMAM G-3 (20 mg/kg), heparin (200 U/kg), and saline on total blood loss caused by tail transection (Fig. 3*G*). Mean blood loss caused by tail injury for over 10 min was 18 µL in normal saline-treated mice ($n = 11$) versus 19 µL in PAMAM G-3–treated mice ($n = 10$). No significant difference in blood loss was observed between saline-treated and PAMAM G-3–treated mice ($P = 0.48$). Taken together with the observations obtained in carotid artery injury assay, these results suggest that PAMAM G-3 prevents thrombus formation without increasing bleeding. By contrast, heparin (200 U/kg) treatment of mice results in significant bleeding following tail transection (saline versus heparin treatment, 18 µL versus 69 µL). Elsewhere, it has been reported that the same concentration of heparin is required to maintain artery patency in mice treated with $FeCl_3$, suggesting that the commonly used anticoagulant heparin can induce severe bleeding when utilized at the dose required to inhibit thrombosis in carotid artery damage model (25). These outcomes suggest that PAMAM G-3 is an anticoagulant that can be used with a reduced risk of bleeding. These results also underscore the important role that naturally occurring extracellular polyphosphates such as DNA, RNA, and inorganic polyphosphates play

in thrombosis, but the limited role that they appear to play in maintaining normal hemostasis.

Discussion

Taken all together, these in vivo observations suggest that the NABP PAMAM G-3 can inhibit coagulation and thrombosis without greatly increasing the propensity to bleed. Because PAMAM G-3 and other existing NABPs were not engineered to be antithrombotic agents, we fully anticipate that ample opportunities now exist to engineer novel NABPs with improved extracellular polyphosphate-scavenging properties and reduced toxicities compared to the currently available NABPs. Nucleic acid-binding polymers have been extensively studied for their function as carriers of different drugs, nucleic acids, and small molecules. Because our studies indicate that nucleic acid-binding polymers such as PAMAM exhibit antithrombotic activity in vivo, such polymers should be evaluated for their effects on coagulation during their therapeutic development.

Regardless, our results with PAMAM G-3 demonstrate the potential utility of NABPs as anticoagulants for treating various thrombotic pathologies as well as their use during various cardiac interventions. We chose two different animal models of thrombosis, arterial ($FeCl_3$-induced carotid artery injury model) and microvascular (collagen/epinephrine-induced pulmonary thromboembolism) to evaluate the antithrombotic effect of PAMAM G-3. The carotid artery injury model is widely used to assess thrombosis in large vessels as a model for myocardial infarction and thrombotic stroke. By contrast, thrombosis in the microvasculature is often evaluated in animals using the collagen/epinephrine-induced pulmonary thromboembolism model we employed. Therefore, in this manuscript we determined that PAMAM G-3 not only inhibited thrombosis in large vessels, such as in a damaged carotid artery, but also had antithrombotic effects in the microvasculature.

A major unmet clinical need exists for developing improved antithrombotic agents because the anticoagulants currently utilized may also cause side effects such as severe and fatal bleeding, adverse immunological responses, and thrombocytopenia, as well as have unpredictable pharmacokinetics (23, 24, 26). We observe that at concentrations that limit thrombosis, PAMAM G-3 does not significantly increase bleeding in a murine tail-transection model. The most likely explanation for this observation is that PAMAM G-3 is inhibiting polyphosphates and nucleic acids from inducing thrombosis by limiting their ability to activate factors XI and XII (10–16). Recent studies on factor XII- and XI-deficient mice demonstrate that these factors appear to be important for thrombosis yet less important for normal hemostasis (27, 28). Thus, PAMAM G-3 may achieve its anticoagulant effect without greatly increasing bleeding by limiting activation of factor XII and XI. Though the clinical development of any novel therapeutic strategy is challenging, it will be interesting to determine if by scavenging extracellular nucleic acids and other polyphosphates, NABPs represent a new and safer approach to control coagulation and limit thrombosis in patients undergoing cardiac interventions, such as percutaneous coronary intervention and coronary artery bypass graft surgery, or who require chronic anticoagulation therapy for limiting pathologic conditions, such as venous thromboembolism, myocardial infarction, stroke, and cancer-induced thrombosis. Future studies that evaluate the pharmacology and toxicology of NABPs for treating thrombotic diseases as well as efforts to engineer novel NABPs for such applications are warranted.

Materials and Methods

Isothermal Titration Calorimetry. ITC was conducted using a MicroCal VP-ITC calorimeter, as described elsewhere (16).

Clotting Assay. Polyphosphates (approximately 60 mer and 130 mer; Regene-Tiss Inc.). were added to 50 μL of normal pooled human plasma (George King Bio-Medical Inc.). and the reaction was incubated at 37 °C for 3 min. Normal saline or PAMAM G-3 (Sigma-Aldrich) was added and the reaction was incubated at 37 °C for 3 min, followed by the addition of 50 μL $CaCl_2$ (25 mM). Clotting times were recorded using STart® Hemostasis Analyzer (Diagnostica Stago).

aPTT and PT assays. aPTT assays and PT assays were performed using TriniCLOT aPTTs (TrinityBiotech) and TriniCLOT PT Excel (TrinityBiotech), respectively, following supplier guidelines. Clotting times were recorded using STart® Hemostasis Analyzer (Diagnostica Stago).

Thrombelastography. Freshly withdrawn blood (320 μL) from healthy human donors was incubated with polyphosphates at 37 °C for 5 min, followed by the addition of dendrimer PAMAM G-3 or normal saline. The reaction was incubated at 37 °C for 5 min and 20 μL $CaCl_2$ (200 mM) was added. Clot formation was recorded using TEG 5000 Thrombelastograph (Haemoscope Corporation) analyzer for 45 min. The whole procedure was approved by the Institutional Review Board of Duke University (Durham, NC).

Carotid Artery Injury Assay. Animal procedures were performed using 10–14-wk-old wild-type female C57BL/6J mice (Jackson Laboratory). Mice were induced by gas inhalation (5% Forane; Baxter). Mice were then intubated and mechanically ventilated (rodent ventilator 683; Harvard Apparatus) with maintenance of anesthesia by 2–2.5% Forane during procedure. Mice were injected with PAMAM G-3 or normal saline into the lateral tail vein in a total volume of 200 μL. Right common carotid artery was exposed. A transonic laser 0.5-PSB transit-time flow probe (Transonic Systems Inc.). was placed around the artery to measure the blood flow. Two small pieces of filter paper (1 mm by 2 mm) saturated with 2.5% $FeCl_3$ were placed on both sides of the carotid artery for 3 min (25). Filter papers were removed and blood flow was monitored for more than 40 min using TS420 perivascular flowmeter (Transonic Systems) and LabChart software (ADInstruments). All experimental protocols involving animals were approved by the Duke University Institutional Animal Care and Use Committee (Durham, NC).

Pulmonary Thromboembolism. Mice were anesthetized using the same method described above. Mice were injected with PAMAM G-3 or normal saline into the left retro-orbital plexus. After 30 min, a mixture of collagen (0.8 mg/kg; Chronolog) and epinephrine (60 μg/kg; Hospira) was injected via right retro-orbital plexus. Mice were carefully observed for respiration to report survival time after the injection of collagen/epinephrine.

Tail-Bleeding Assay. Mice were anesthetized using the same method described above. PAMAM G-3, heparin (APP Pharmaceuticals), or normal saline was delivered to mice via retro-orbital plexus. After 15 min, 3 mm of distal mouse tail was removed and the tail was immediately immersed in 1 mL isotonic saline (37 °C). Blood was collected for 10 min after tail transection. The total blood loss was determined by measuring the absorbance of the blood containing normal saline at 560 nm, as described elsewhere (29). A standard curve method was used to calculate the total blood loss caused by tail transection. All experimental protocols involving animals were approved by the Duke University Institutional Animal Care and Use Committee (Durham, NC).

ACKNOWLEDGMENTS. We thank Jens Lohrmann, Maureane Hoffman, and Shahid Nimjee for technical help and Richard C. Becker for useful discussions. This study was supported in part by funds from National Heart, Lung, and Blood Institute (HL065222).

1. Moscucci M (2002) Frequency and costs of ischemic and bleeding complications after percutaneous coronary interventions: Rationale for new antithrombotic agents. *J Invasive Cardiol* 14:55B–64B.
2. Mannucci PM, Franchini M (2011) Old and new anticoagulant drugs: A minireview. *Ann Med* 43:116–123.
3. Spyropoulos AC (2008) Brave new world: The current and future use of novel anticoagulants. *Thromb Res* 123(Suppl 1):S29–S35.
4. Roger VL, et al. (2011) Heart disease and stroke statistics, 2011 update: A report from the American Heart Association. *Circulation* 123:e18–e209.
5. Fanikos J, et al. (2007) Adverse drug events in hospitalized cardiac patients. *Am J Cardiol* 100:1465–1469.
6. Moore TJ, Cohen MR, Furberg CD (2007) Serious adverse drug events reported to the Food and Drug Administration, 1998–2005. *Arch Intern Med* 167:1752–1759.
7. Haas S (2009) New anticoagulants: Towards the development of an "ideal" anticoagulant. *Cor Vasa* 38:13–29.

8. Kannemeier C, et al. (2007) Extracellular RNA constitutes a natural procoagulant cofactor in blood coagulation. *Proc Natl Acad Sci USA* 104:6388–6393.
9. Nakazawa F, et al. (2005) Extracellular RNA is a natural cofactor for the (auto-)activation of factor VII-activating protease (FSAP). *Biochem J* 385:831–838.
10. Fuchs TA, et al. (2010) Extracellular DNA traps promote thrombosis. *Proc Natl Acad Sci USA* 107:15880–15885.
11. Choi SH, Smith SA, Morrissey JH (2011) Polyphosphate is a cofactor for the activation of factor XI by thrombin. *Blood* 118:6963–6970.
12. Smith SA, Morrissey JH (2008) Polyphosphate enhances fibrin clot structure. *Blood* 112:2810–2816.
13. Mutch NJ, Engel R, Uitte DW, Philippou H, Ariens RA (2010) Polyphosphate modifies the fibrin network and down-regulates fibrinolysis by attenuating binding of tPA and plasminogen to fibrin. *Blood* 115:3980–3988.
14. Muller F, et al. (2009) Platelet polyphosphates are proinflammatory and procoagulant mediators in vivo. *Cell* 139:1143–1156.
15. Oney S, et al. (2009) Development of universal antidotes to control aptamer activity. *Nat Med* 15:1224–1228.
16. Lee J, et al. (2011) Nucleic acid-binding polymers as anti-inflammatory agents. *Proc Natl Acad Sci USA* 108:14055–14060.
17. Esfand R, Tomalia DA (2001) Poly(amidoamine) (PAMAM) dendrimers: From biomimicry to drug delivery and biomedical applications. *Drug Discov Today* 6:427–436.
18. Svenson S, Tomalia DA (2005) Dendrimers in biomedical applications: Reflections on the field. *Adv Drug Deliv Rev* 57:2106–2129.
19. Smith SA, et al. (2010) Polyphosphate exerts differential effects on blood clotting, depending on polymer size. *Blood* 116:4353–4359.
20. Malik N, et al. (2000) Dendrimers: Relationship between structure and biocompatibility in vitro, and preliminary studies on the biodistribution of 125I-labelled polyamidoamine dendrimers in vivo. *J Control Release* 65:133–148.
21. Harrington RA, et al. (2008) Antithrombotic therapy for non-ST-segment elevation acute coronary syndromes: American college of chest physicians evidence-based clinical practice guidelines (8th edition). *Chest* 133:670S–707S.
22. Wiviott SD, et al. (2007) Prasugrel versus clopidogrel in patients with acute coronary syndromes. *N Engl J Med* 357:2001–2015.
23. Stone GW, et al. (2007) Antithrombotic strategies in patients with acute coronary syndromes undergoing early invasive management: One-year results from the ACUITY trial. *JAMA* 298:2497–2506.
24. Levi M, Eerenberg E, Kamphuisen PW (2011) Bleeding risk and reversal strategies for old and new anticoagulants and antiplatelet agents. *J Thromb Haemost* 9:1705–1712.
25. Wang X, Xu L (2005) An optimized murine model of ferric chloride-induced arterial thrombosis for thrombosis research. *Thromb Res* 115:95–100.
26. Hirsh J, et al. (2008) Parenteral anticoagulants: American college of chest physicians evidence-based clinical practice guidelines (8th edition). *Chest* 133:141S–159S.
27. Gailani D, Lasky NM, Broze GJ, Jr (1997) A murine model of factor XI deficiency. *Blood Coagul Fibrinolysis* 8:134–144.
28. Pauer HU, et al. (2004) Targeted deletion of murine coagulation factor XII gene: A model for contact phase activation in vivo. *Thromb Haemost* 92:503–508.
29. Fay WP, Parker AC, Ansari MN, Zheng X, Ginsburg D (1999) Vitronectin inhibits the thrombotic response to arterial injury in mice. *Blood* 93:1825–1830.